Table of Contents

List of Figures

1.0 INTRODUCTION

A series of transient analysis using the system code RELAP5/ATHENA [1] has been performed to assess decay heat removal by natural circulation cooling under postulated accident conditions. The analysis is for a helium cooled reactor of pin core design with a power density of 100 W/cc and a thermal power of 2400 MW. The objective is to ensure that the maximum fuel temperature remains within acceptable limits (< 1600°C) following a depressurization accident with scram and total loss of AC power.

The removal of decay heat from the core will follow the initiation of the depressurization accident in two steps. Initially, heat will be removed by a combination of flow coastdown due to inertia of the power conversion system and system depressurization caused by coolant flowing out of the break from the primary system. Following this step a self-sustaining method for long-term heat removal of the core will be required. A passive mode of heat removal relying on natural circulation cooling is investigated in this report. An emergency heat exchanger loop outside the reactor vessel will transfer energy from the reactor to an ultimate heat sink located outside the guard containment. By the opening of a check valve inline with the emergency heat exchanger a natural circulation flow path is established through the core and between the upper plenum and downcomer of the reactor vessel. Radiative heat transfer has also been included in the model to account for the exchange of thermal energy between heat structures by radiation.

In order for natural circulation cooling to function efficiently the primary system and the containment will need to be pressurized to ensure a sufficiently high coolant density. This will be accomplished by having a guard containment structure around the primary system. The main objective of the analysis reported here is to evaluate the effects of guard containment back pressure on the effectiveness of natural circulation cooling.

2.0 RELAP5/ATHENA MODEL

A RELAP5 model of the reactor system has been constructed to address different parametric effects that influence the steady state and transient behavior of the pin core under natural circulation cooling at decay heat power levels. The model consists of two power conversion unit loops, an emergency heat exchanger loop with its heat sink, and a guard containment surrounding the primary system. The actual power plant will be constructed using four power conversion loops. However, in the RELAP model three loops are combined into one large loop (1800 MW), and one loop (600 MW) is isolated in order to correctly model the depressurization dynamics, since the leak flow will emanate from only one of the power conversion loops. This arrangement is shown schematically on Figure 1. Several volumes are used to represent the core and the pressure vessel, and the fuel and metal components are represented as heat structures. Thermal radiation is accounted for between the heat structures. The core has multiple axial and radial channels in order to represent both axial and radial power distributions. The shutdown and emergency cooling system is sized to handle 2% decay heat removal by natural circulation in a 4x50% configuration, i.e. four separate loops of 1% power capacity. In the RELAP5 model the emergency heat removal system is represented by

one heat exchanger, which is sized to handle 2% of full power. Thus, once the decay heat reaches a level of 2 % of full power the emergency heat removal system should be able to handle the heat load. The heat exchanger is based on the compact HEATRIC concept. The primary side coolant is helium, which is used to cool the core, and the secondary side uses pressurized water as a working fluid. The ultimate heat sink consists of a large water tank located outside the guard containment building.

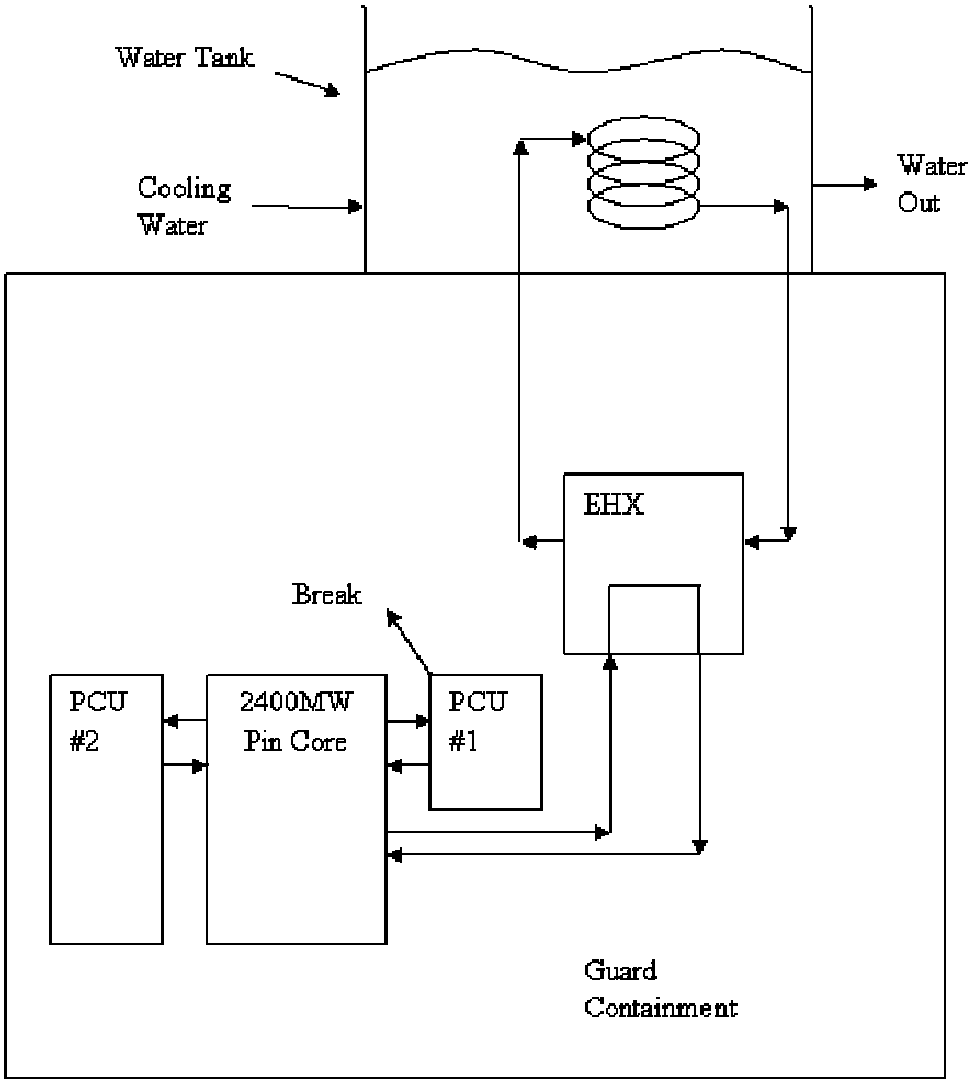

Figure1 – Schematic Model of the Reactor System and the Associated Emergency Cooling Loop.

Details of the heat structures used in the RELAP model for convective and radiative heat transfer are shown in Figure 2. The core model consists of three radial zones and ten axial zones. The three radial zones include a hot assembly, a hot zone, and an average zone.

Each of the radial zones is divided into ten axial zones. Power generation in each zone is obtained from output of the reactor physics analysis. Beyond the core there is a radial reflector, shield, core barrel, reactor pressure vessel wall and support structure, and finally the guard containment wall. It is seen that explicit heat generation is only modeled in the core volumes. Heat generation in the other volumes is of marginal importance, and these structures act only as thermal capacitors.

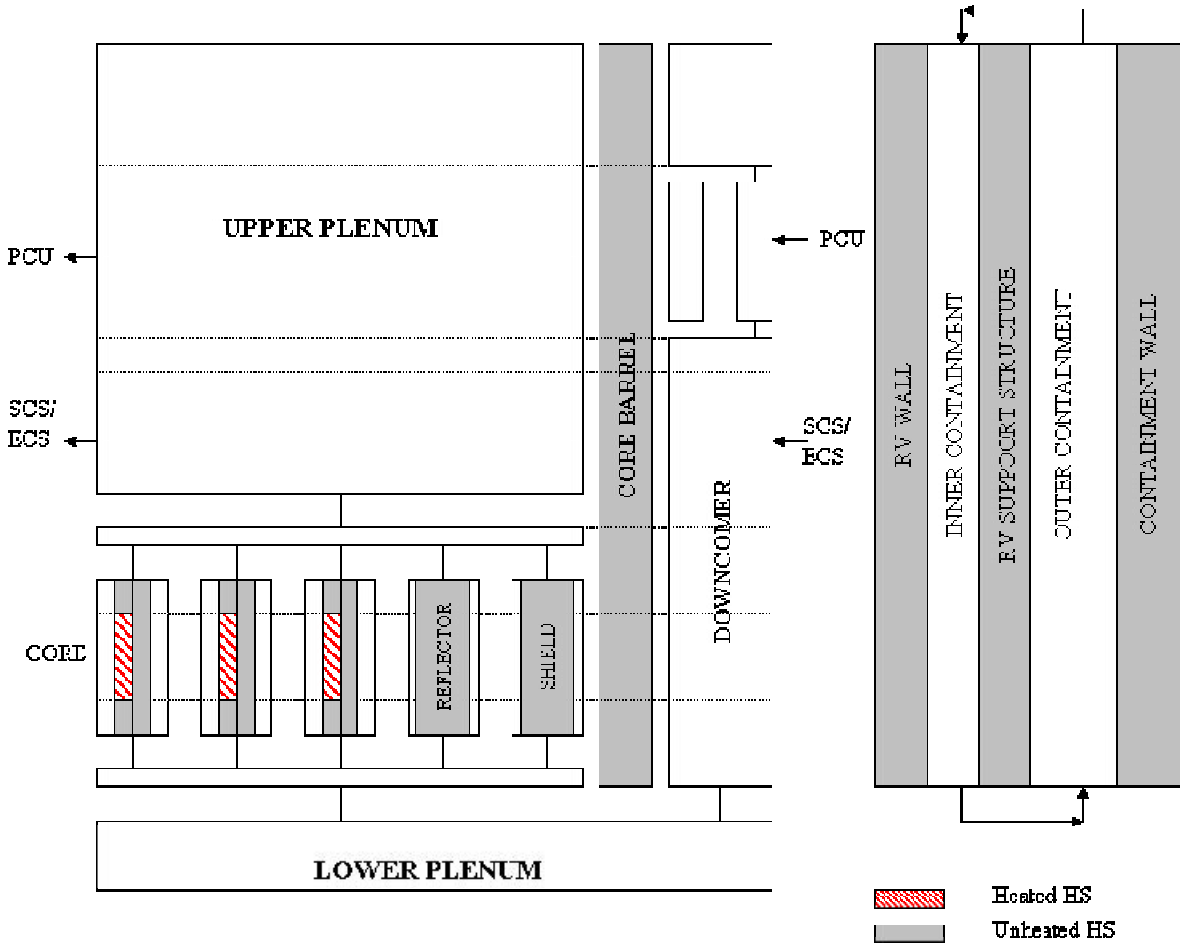

Figure 2 – Reactor Vessel and Guard Containment Heat Structures.

The model for determining the heat transfer due to radiation is shown in Figure. 3. This model allows for radial radiation heat transfer only, and couples the hot inner core parts to the cooler outer parts. Figure 3 is thus a radial section through the core and associated guard containment wall, since these are the heat structures involved in the heat transfer process. It is seen that the fuel pins radiate to the assembly cans, which in turn radiate to each other. At the outer core boundary the element cans radiate to the inner reflector surface, which radiates to the radial shield. Finally the shield radiates to the core barrel, which radiates to the reactor pressure vessel, and it finally radiates to the guard

containment wall. It is assumed that the guard containment wall is kept at a constant temperature by a thermal management system embedded in the wall.

It is clear from the above discussion that the core heat transfer model has both a convective and a radiative component. Convectively, heat is removed from the core by helium gas flowing up along the fuel pins. This mechanism is either forced or natural convection. The second heat transfer mechanism is radiation from the hotter parts of the core to the cooler parts of the core.

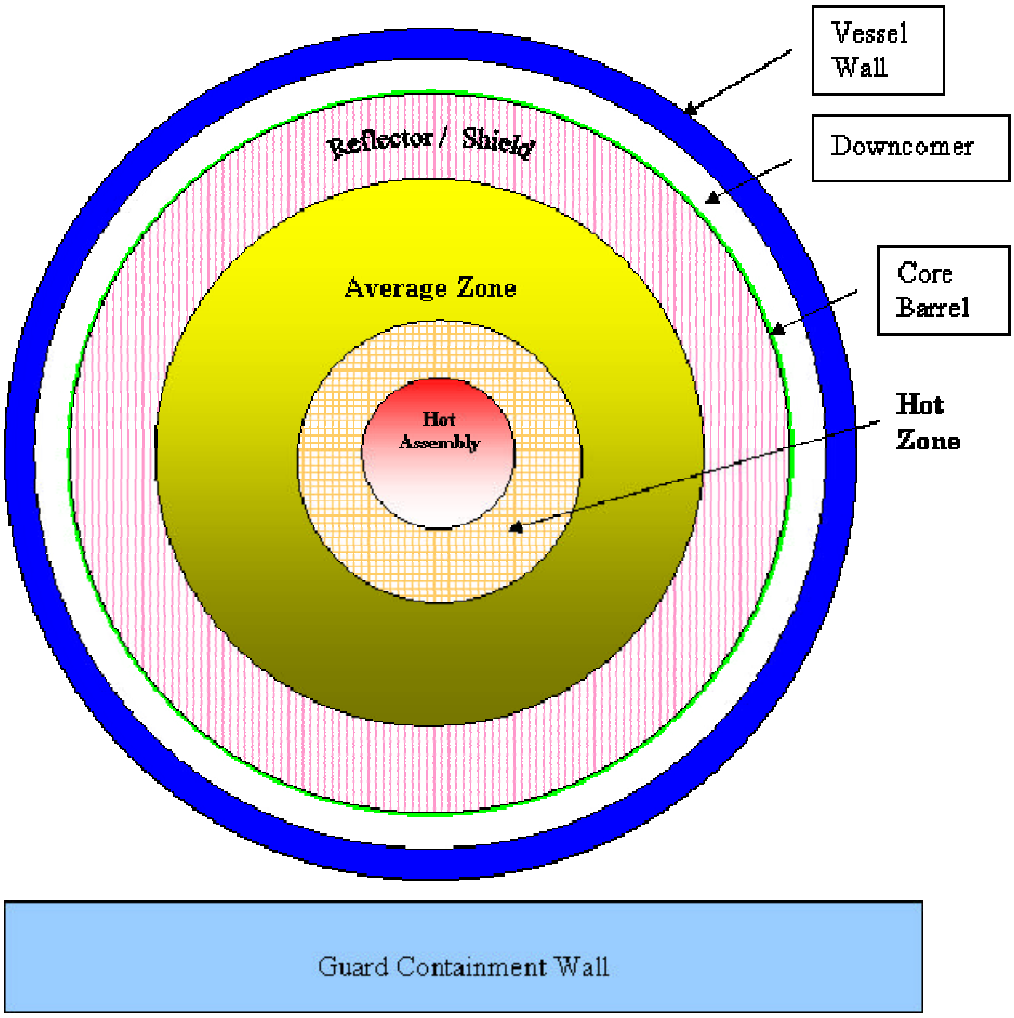

Figure 3 – Heat Structures for Radiation Heat Transfer.

Details of the primary system and the power conversion unit (PCU) are shown in Figure 4. It is seen that all the components of the power conversion unit are represented. However, at this stage the actual turbine, compressors, and generator models are not complete. The actual models for these components, including performance maps and inertia terms, will be added at a later date. The primary system depressurization is

assumed to take place from a failure in the cold inlet duct of the primary circuit. This location is close to the point of highest primary system pressure (actually located at the exhaust of the high pressure compressor outlet). Also shown in Figure 4 is the guard containment structure into which the primary coolant exhausts at the time of the break.

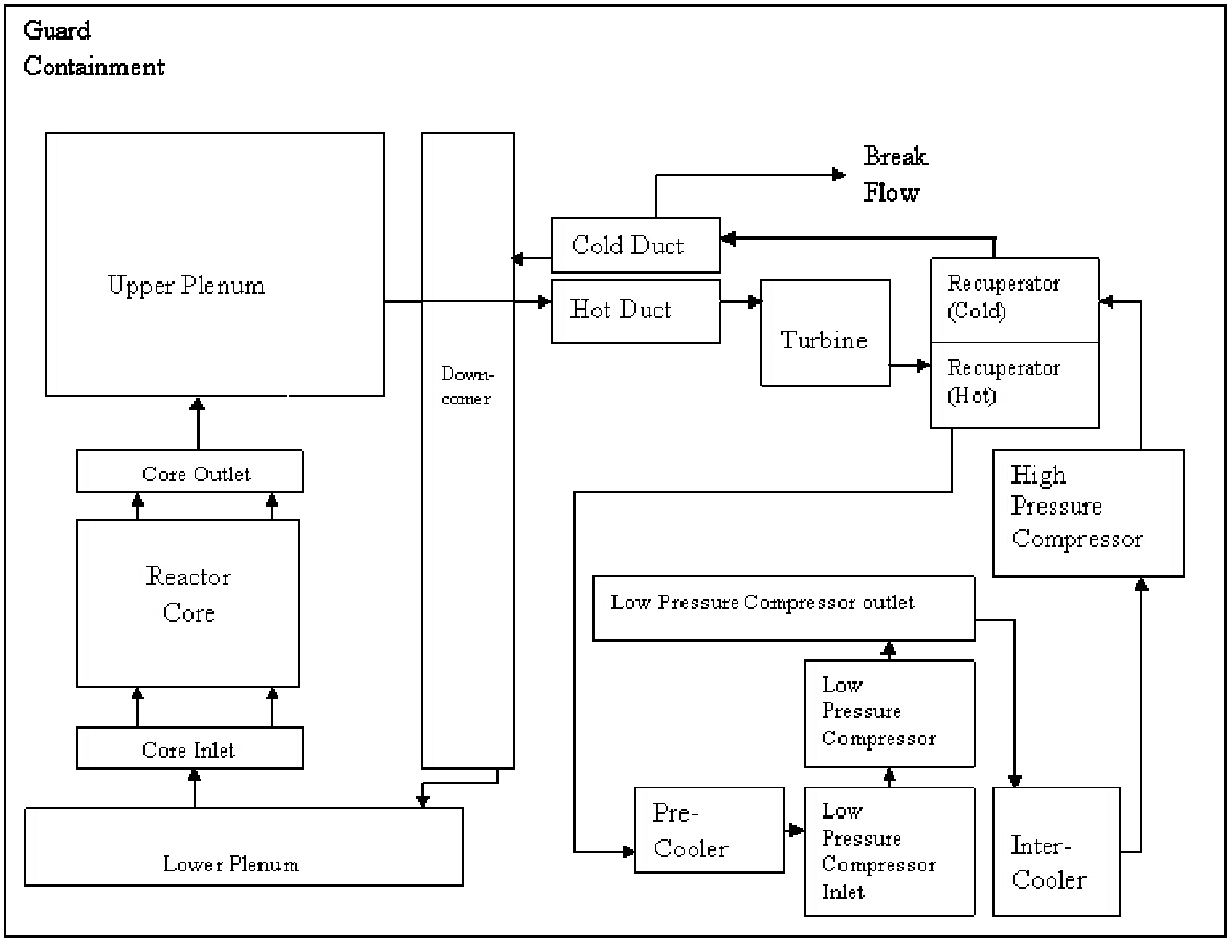

Figure 4 – Reactor Vessel and Power Conversion Unit Volume arrangement.

Details of the volume representation of the Shutdown Cooling System/Emergency Cooling System (SCS/ECS) are shown in Figure 5. The intermediate heat exchanger is based on the HEATRIC concept, and is shown in the horizontal orientation. A vertical orientation was also examined in the series of analysis reported below. The inlet and outlet of the SCS/ECS loop is connected to the upper plenum and the downcomer of the reactor pressure vessel respectively. Although the blower volume is explicitly modeled, the actual blower rotating components are not included at this stage. The inertia of the drive motor and/or the possible availability of backup battery power both of which could assist in forcing coolant to circulate around the primary circuit are thus not included in this analysis. This capability will be included in the next stage of the analysis.

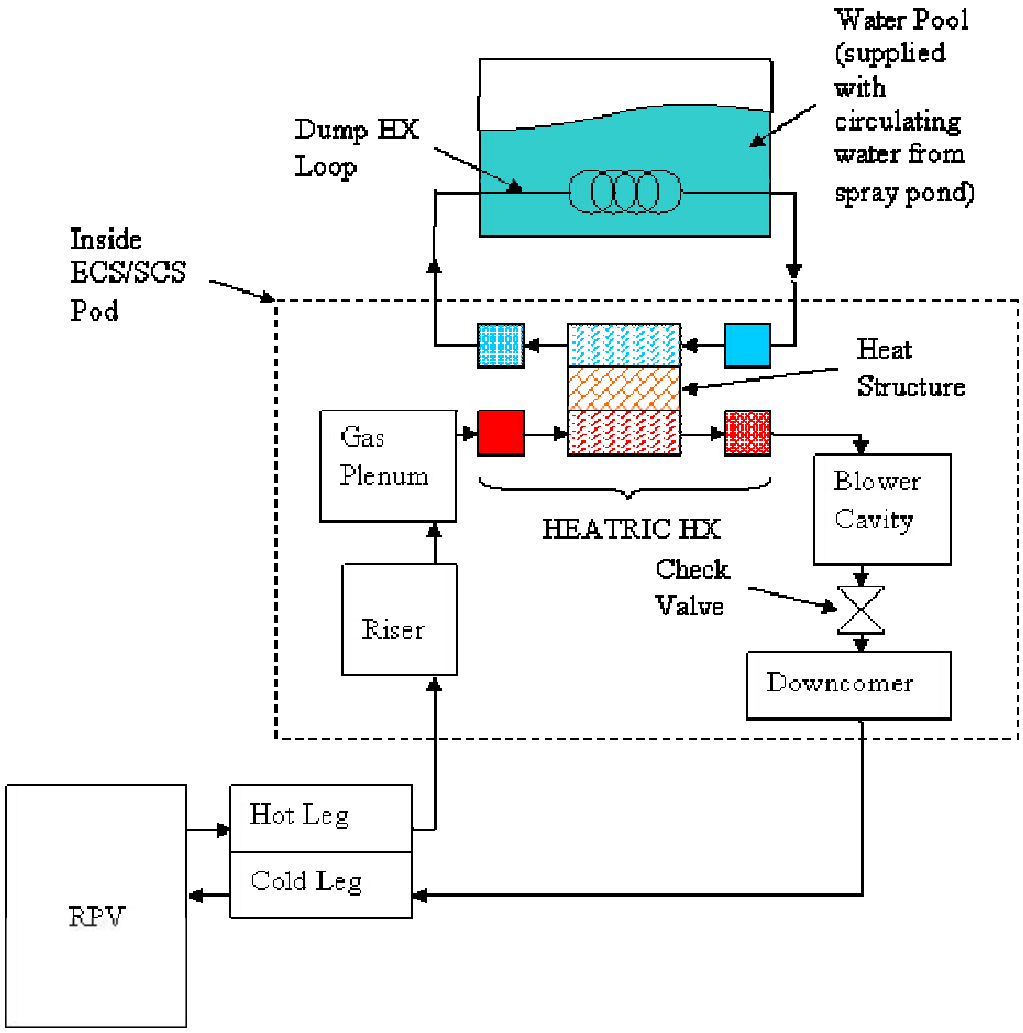

Fig. 5 – Shutdown Cooling System/Emergency cooling System Volume arrangement.

2.1 Reactor Model for Steady-State Initialization

As shown in Figure 4, the RELAP model represents an integrated depiction of the primary and power conversion loops. Table 1 provides a summary of the geometric parameters of the inter-connecting volumes that represent different parts of the reactor vessel and Table 2 provides the geometry and initial conditions for one unit of the 600MW PCU.

The following is a list of reactor parameters used in the model and is based on the ANL input database for the core design [2].

Reactor power = 2400 MWt
System pressure = 7.0 MPa

Core $\Delta P = 5.2 \times 10^4$ Pa
Helium flow = 1249 kg/s
Inlet temperature = 480°C
Outlet temperature = 850°C

The corresponding fuel subassembly parameters are listed in the following.

Number of hexagonal subassemblies = 418 (including 61 control assemblies)
Number of fuel pins per subassembly = 271 (234 in control assemblies)
Pin diameter = 9.65 mm [3]
Clad (SiC) thickness = 1.0 mm [3]
Radial gap (helium) = 0.1 mm [3]
Fuel pellet (UC) diameter = 7.45 mm [3]
Total coolant flow area = 9.1 m^2
Channel height = 3.34 m (fissile height = 1.34m)
Hydraulic diameter = 12.2 mm
Number of spacer grid assumed = 9
Spacer grid loss coefficient = 0.65
Flat-to-flat (outside) of hexagonal subassembly = 215 mm
Hexagonal wall thickness = 3.7 mm

Thermal properties of UC and SiC used in the analysis are listed in Table 3.

Preliminary physics calculation from ANL [3] indicated that reactor power is distributed between the core and the radial reflector/shield in a ratio of 99.65 % : 0.35 %. Since the energy deposition outside the core is negligible 100% of power is assumed to deposit in the three core zones. A flow split of 99.65% : 0.35% is assumed between the core and the radial reflector/shield. The reactor core is divided into a hot assembly, hot zone, and an average zone. The pertinent parameters associated with these zones are given below:

	Hot Assembly	Hot Zone	Average Zone
Number of Assemblies:			
Regular Assembly	6	48	303
Control Assembly	0	7	54
Power Fraction (%)	1.7	14.1	84.2
Relative Radial Power Shape	1.31	1.21	0.967

The inclusion of the hot assembly as one of the three zones in the core is to simulate the effect of pin peaking within the hot zone. The assumed peaking is ~8% ((1.31-1.21)/1.21). Each region is sub-divided into 10 axial nodes with mid-core symmetry and a cosine axial power shape. The bottom and top nodes represent the axial reflectors (1 m in length) and no heat generation is assumed there. The axial power factors in the fueled region, from inlet to mid-core are: 0.82 (0.101m), 0.91 (0.168m), 1.04 (0.202m), 1.12 (0.202m), where the length of each node is in parenthesis. The fuel pins are modeled as cylindrical heat structures with three radial zones, fuel, gas gap, and clad. In parallel with the core channels is the radial reflector/shield volume with its own hydraulic channel and

heat structure. Details of these passive heat structures (no internal heat generation) are discussed later in relation to the modeling of radiation heat transfer.

2.2 Emergency Heat Exchanger System

Under natural circulation cooling decay power is removed by an in-vessel heat exchanger of HEATRIC design. A secondary loop using pressurized water transports the thermal energy, again by natural circulation, to an externally located ultimate heat sink. For this analysis the emergency heat exchanger system is modeled after an MIT design, shown in Figure 5. The HEATRIC heat exchanger consists of alternating layers of helium and pressurized water counter-current micro-channels. The HEATRIC heat exchanger is represented in the RELAP5 model as a plate heat structure separating the counter-current primary and secondary fluids. The secondary heat exchanger, located in the ultimate heat sink, consists of a tube and shell design with ten tube passes and one shell pass. The shell side is a water tank that represents an ultimate heat sink. The tank is assumed to be very large, and if necessary can be refilled. Design data relevant to the RELAP5 model are shown in Attachment 1. Below is a summary of the heat exchanger input data.

Working fluid = H_2O pressurized to 9 MPa
Length of heat transfer surface = 0.3m
Plate thickness = 0.0037m
Heat transfer area = 2360m^2
Flow area on the primary and secondary side = 6.01m^2
Hydraulic diameter of flow channel = 0.003055m
Plate conductivity is based on Alloy 800H,

$K_{mat}(T) = 6.8393 + 0.015577T$,

where K_{mat} is the thermal conductivity in W/m-s and T is the temperature in K.

The arrangement of the SCS/ECS heat exchanger as it is located in a pod in the guard containment is shown in Fig. 6.

The following additional assumptions were made regarding the operation of the emergency cooling system:

1) The HEATRIC flow channels were oriented in the vertical direction. The original design had horizontal flow channels. However initial calculations showed a period of steam void formation at the start of heat transfer to the water side. For the calculations presented in this report the flow channels were oriented vertically to ease the establishment of natural circulation flow on the water side.
2) The difference in height between the core mid-plane and the mid-plane of the emergency heat exchanger is 16 m.
3) The height between the emergency heat exchanger mid-plane and the tube heat exchanger mid-plane located in the ultimate heat sink is 8.5 m.

4) The ultimate heat sink tank is supplied by an external water supply at a rate of 355.2 kg/s at a temperature of 30° C.
5) The external water tank, representing the shell side of the secondary heat exchanger, is open to atmosphere and is assumed to have a height of 10m and a flow area of 78.54m^2.
6) The tube side of the secondary heat exchanger is made up of 100 tubes with ID = 0.03505m, OD = 0.04216 and10 tube passes. Total flow area = 0.09649m^2 and total heat transfer area = 425.14m^2 (total heat transfer length = 10x3.21m).

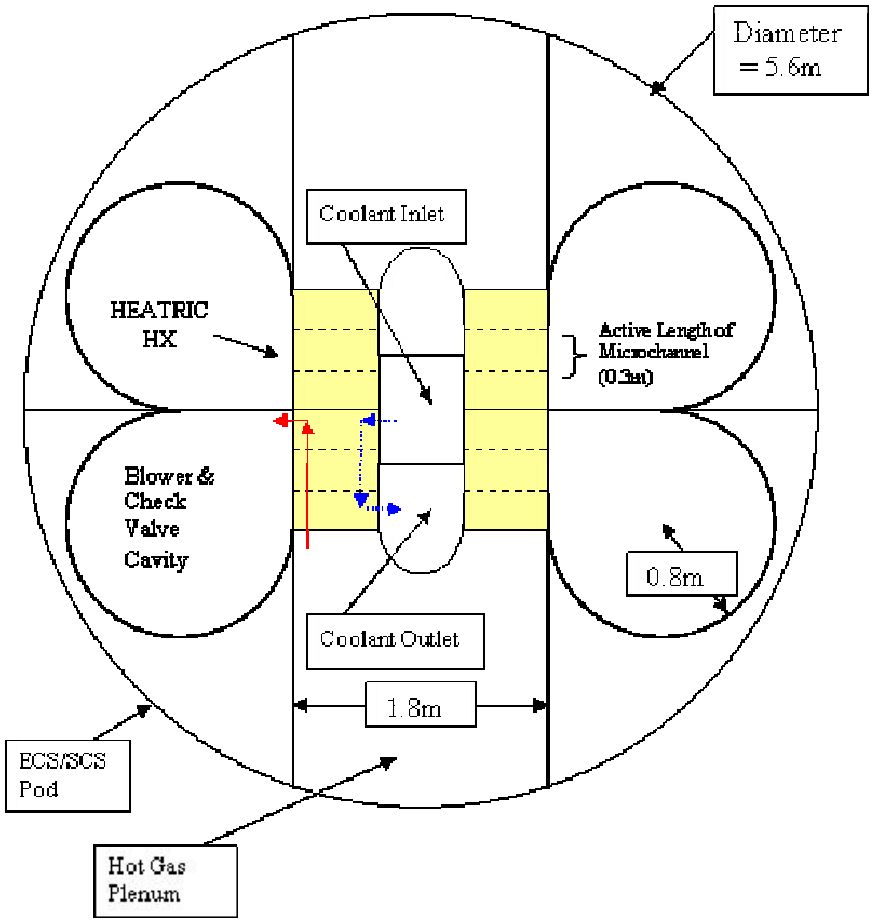

Fig. 6 – SCS/ECS heat exchanger located in a pod within the guard containment.

2.3 Radiative Heat Transfer

The incorporation of radiation heat transfer among heat structures inside the reactor vessel provides an additional means of distributing thermal energy from hotter parts to cooler parts of the reactor. A simplified approach that is consistent with the lumped representations of fuel pins and assembly cans has been adopted to model the transfer of

heat by radiation from fuel pins to the surrounding assembly cans and subsequently from one zone of the core to the next.

The heated heat structures (HS), i.e. the fuel pins, identified in Figure 2 is the source of energy and the unheated heat structures are other components that participate in the exchange of thermal energy by radiation. By assumption the zone of influence of radiation heat transfer is limited to the cylindrical section that coincides with the vertical extent of the fueled region of the core. As an example, though the core barrel extends to the upper plenum, only the lower portion between the lower and upper boundaries of the fueled zone (1.347m in height) participates in radiation heat transfer.

The corresponding radiation heat transfer surfaces considered in the ATHENA model of the pin core are:

1. Fuel pins in each core zone (hot assembly, hot zone, and average zone, as shown in Figure 3) radiate to the corresponding hexagonal (hex) cans in the zone.
2. Hot assembly hex can radiates to hot zone hex can.
3. Hot zone hex can radiates to average zone hex can.
4. Average zone hex can radiates to radial reflector.
5. Radial reflector radiates to radial shield.
6. Radial shield radiates to core barrel.
7. Core barrel radiates to vessel wall.
8. Vessel wall radiates to vessel support structure.
9. Vessel support structure radiates to guard containment wall.

Once the radiating surfaces have been identified the other parameter of interest for radiation heat transfer is the view factor. In ATHENA the two rules that govern the definition of view factors for two interacting surfaces are:

$A_i F_{ij} = A_j F_{ji}$

$\Sigma F_{ij} = 1$ (For a given i sum over j)

where,

A_i = area of radiating surface i
F_{ij} = view factor from surface i to surface j

In this report the view factors for a given pair of radiating surfaces (A_i and A_j) are evaluated by assuming that the two surfaces are two-dimensional concentric cylinders. According to the conceptualized radiating surfaces shown in Figure 3, the inner cylinder (A_1) sees 100% of the outer cylinder (A_2) and this gives F_{12} =1 that enables the determination of the rest of view factors for the pair of surfaces A_1 and A_2. The situation for radiative transfer between the fuel pins and the surrounding hex can walls is a little different. In this case the fuel pins have a total surface area (A_1) greater than the corresponding surface area of the hex cans (A_2) and F_{21} is set to unity instead. Physically

the interpretation of setting F_{21} =1 (hex can to fuel pin) is equivalent to treating the hex can as seeing 100% of the fuel pins while the fuel pins only see part of the hex can surface because the fuel pins see each other. This interpretation is consistent with the use of one lumped fuel pin to represent all the fuel pins in a core zone, i.e. fuel pins radiate to each other to achieve the same temperature at each axial location in a particular core zone.

Some of the input parameters for the heat structures that participate in radiation heat transfer are summarized below.

Radial reflector:
Inner radius = 2.4265m
Outer radius = 2.6955m
Material = Inconel

Radial shield:
Inner radius = 2.8175m
Outer radius = 3.2785m
Material = Inconel

Core barrel:
Inner radius = 3.355m
Outer radius = 3.38m
Material = stainless steel

Reactor vessel wall:
Inner radius = 3.6856m
Outer radius = 3.965

Reactor support structure:
Inner radius = 5.77m
Outer radius = 6.67m
Material = concrete

Guard containment wall:
Wall thickness = 0.02m
Material = concrete
An arbitrarily thin wall was used to simulate a wall that is close to the temperature of the outside temperature of 30 deg C. The boundary condition prescribed for the guard containment wall is an approximation to the design assumption that the guard containment wall is kept at a constant temperature by a thermal management system embedded in the wall.

The transient results indicate that the main effect of radiative heat transfer is the redistribution of energy among heat structures internal to the vessel. Radiative heat

transfer to the guard containment wall is insignificant because of relatively low reactor vessel wall temperature.

2.4 Transient Boundary Conditions and Cases

In order to carry out a transient analysis of a thermal-hydraulic system both initial and boundary conditions need to be specified. In the cases to be considered here the following conditions will be specified:

1) Reactor initially at full power.
2) A 0.00645 m^2 (1.0 in^2) rupture in the number one loop (600 MW) of the PCU cold leg initiates the transient.
3) Appropriate volumes represent power conversion unit, but no actual turbo-compressor model is included in the model.
4) Transient response of the turbo-compressor unit is modeled by linearly reducing the flow from the PCU into the primary loop. A ramp down time of 180 s. was assumed.
5) Guard containment volume is an input variable the magnitude of which is to be determined by the results of the transient analysis. Initially pressure and temperature were assumed to be 1 atmosphere and 30º C. The guard containment outside wall temperature was assumed to be at a steady state value of 30º C. It is assumed that the temperature is maintained by an outside independent heat removal system.

The primary objective of this analysis is to determine the volume and final temperature and pressure of the guard containment that result in acceptable core long term cooling of the core. Acceptable cooling of the core is defined by the conditions that result in the maximum hot pin surface temperature being below 1800 K. By varying the guard containment volume the final pressure in the guard containment also varies, and this value determines the density and thus the mass flow rate of the coolant flowing through the core. Higher guard containment pressures result in higher coolant mass flow rates and thus more efficient cooling. However, they also imply thicker guard containment walls and thus potentially more costly structures.

3.0 ATHENA TRANSIENT ANALYSIS

The first step of a transient analysis was to establish a steady-state at 100% power. The current models of the PCU do not include a compressor component and so initial flow is established by imposing upstream and downstream pressures in the reactor vessel, given the system pressure of 7.0MPa and a core pressure drop of 5.72×10^4Pa. With a helium inlet temperature of 480°C, the spacer loss coefficient is adjusted until an outlet temperature of 850°C is reached at the outlet of the reactor.

A transient case is run as a restart of the steady-state case from time zero. Simultaneously the restart case establishes new connections to the RPV at time zero. These include new flow junctions with the PCU via the cold and hot ducts and the guard containment via the

break junction (simulated by a trip valve). Specifically the restart input file contains information for the break junction (flow area), the guard containment (volume, initial pressure and temperature), the PCU initial pressure and temperature distribution, time-dependent junction velocity between PCU and RPV inlet to simulate forced flow coastdown. The coast-down of forced flow is simulated by varying the junction flow velocity linearly from the initial value to zero in a specified time period. The nominal coastdown period is 180 seconds. At the end of the coastdown, a valve is tripped open to provide a flow path between the PCU outlet and the downcomer of the reactor. The break is initiated at time zero of a transient case and the reactor is tripped on an upper plenum pressure of 6.0MPa. Reactor power after scram is calculated by the RELAP5 point-kinetics model and the fission product decay information specified is ANS79-1.

3.1 Transient Cases

A series of transient analysis has been done to evaluate the effect of guard containment pressure on the passive mode of decay heat removal by natural circulation cooling. The effect of back pressure on natural circulation cooling of the pin core is evaluated by parametrically varying the free volume of the guard containment. The nominal case (Case 1) has an assumed guard containment volume of 27000 m^3 and a final calculated pressure of 0.574MPa. The other cases have volumes and final pressures as shown below.

Case Identification	Guard Containment Free Volume (m^3)	Final Containment Pressure (MPa)
Case 1	27000 (Nominal)	0.574
Case 2	0.5 x Nominal	0.901
Case 3	1.33 x Nominal	0.472
Case 4	0.75 x Nominal	0.675

Only two of the four cases resulted in an end state whereby natural circulation cooling has sufficient capacity to remove decay heat generated by the 2400 MW core. The results indicate that the guard containment back pressure has a dominant effect on the rate of heat removal by natural circulation with higher pressure leading to higher flow rate. Results of each parametric case and an analysis of the transient results for all four cases considered together are provided in the following sections.

3.1.1 Case 1

This case assumes the guard containment has a nominal free volume of 27000m^3. Maximum fuel temperature in the hot channel exceeded 1600°C at about 14350s after initiation of the break (see Figure 12). At that time the pressures in the reactor and the guard containment have equilibrated to about 0.57MPa (see Figure 9).

3.1.2 Case 2

This case has a guard containment free volume of 13500 m^3 (half that of the nominal value). Pressures in the reactor and the guard containment converge to about 0.9MPa (see Figure 9) at the end of the calculation, 21600s after initiation of the break. The emergency heat exchanger is able to match the decay power (see Figure 7) and the maximum fuel temperature of 1274.4K is reached at 13540s (see Figure 12).

3.1.3 Case 3

This case assumes a guard containment volume of 36000 m^3, a third larger than the nominal volume. The outcome is similar to Case 1. Maximum fuel temperature in the hot channel exceeded 1600°C at 13967s after initiation of the break (see Figure 12). At that time the pressures in the reactor and the guard containment have equilibrated to about 0.47MPa (see Figure 9).

3.1.4 Case 4

This case has a guard containment free volume of 20250 m^3 (0.75 that of the nominal value). Pressures in the reactor and the guard containment converge to about 0.675MPa (see Figure 9) at the end of the calculation, 24000s after initiation of the break. The emergency heat exchanger is able to match the decay power (see Figure 7) and the maximum fuel temperature of 1736.9K is reached at about 22700s (see Figure 12).

3.2 Analysis of Transient Results

The general progression of the depressurization transient for the four parametric cases is very similar and the transient results for all four cases are plotted together to facilitate comparison of trends.

3.2.1 Heat Removal Rate of the Emergency Cooling System

Plotted in Figure 7 is the rate of heat transfer into the water side of the HEATRIC heat exchanger in the emergency cooling system. The reactor power also is shown in the figure for comparison.

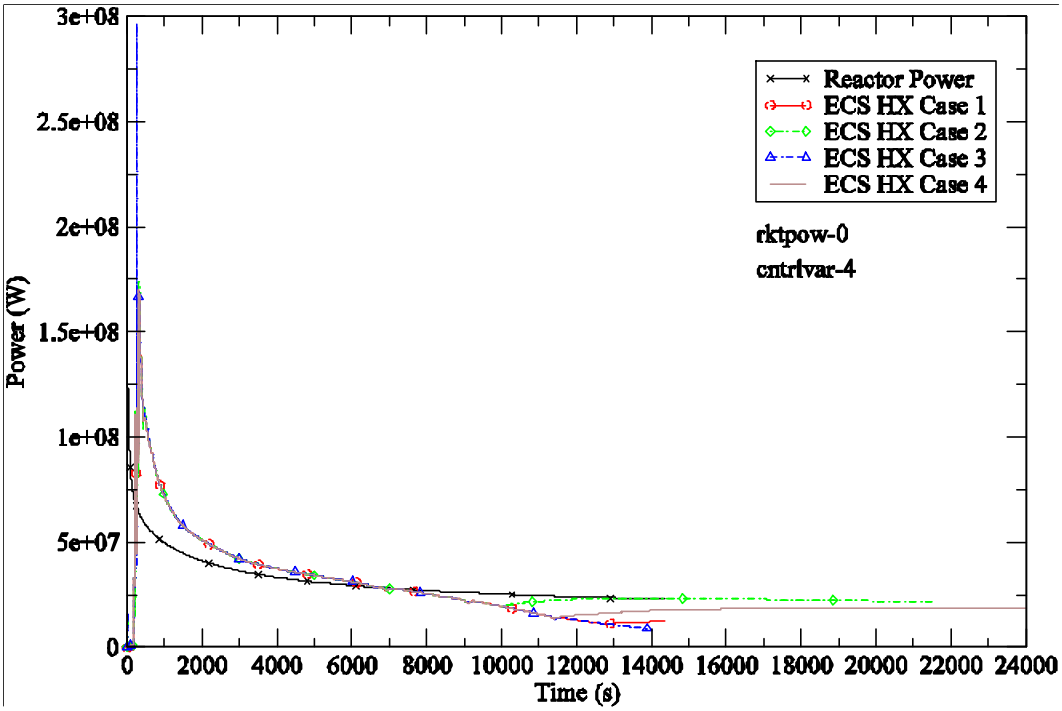

Figure 7 – Reactor power and Emergency Heat Exchanger heat removal rate.

The initial surge in the heat removal rate is due to the hydraulic transient on the water side of the heat exchanger (see Figure 15). A comparison between Figures 7, 8 and 9 shows that as the reactor pressure comes into equilibrium with the guard containment pressure, indicating an end to the depressurization phase of the transient, there is a slow migration of the heat exchanger heat removal rate towards the reactor power. This trend is indicative of the approach to a quasi-steady state where the natural circulation heat removal rate matches that of the reactor power.

3.2.2 Reactor Pressure

The pressure of the reactor upper plenum is shown in Figure 8. With the initiation of the break at time zero, the current RELAP5/ATHENA model assumes a linear coastdown of flow velocity from the power conversion unit (PCU) to the reactor. This is an interim scheme to simulate the behavior of a tripped PCU until a compressor/turbine model is developed for a more realistic representation of the PCU. The mean initial pressure of the PCU is less than the reactor pressure. With no rotating machinery in the current model to provide hydraulic head in the PCU, helium gas in the reactor quickly depressurizes into the PCU volumes. This results in a rapid drop in reactor pressure at time zero. The rest of the depressurization is more gradual and is due to leakage through the break into the guard containment. For much of the depressurization transient the helium flow through the leak is choked and thus all four parametric cases have similar reactor pressure until the point the reactor pressure equalizes with the guard containment pressure. In the two failed cases (Cases 1 and 3) the peak clad temperature exceeds the limit of 1600°C after

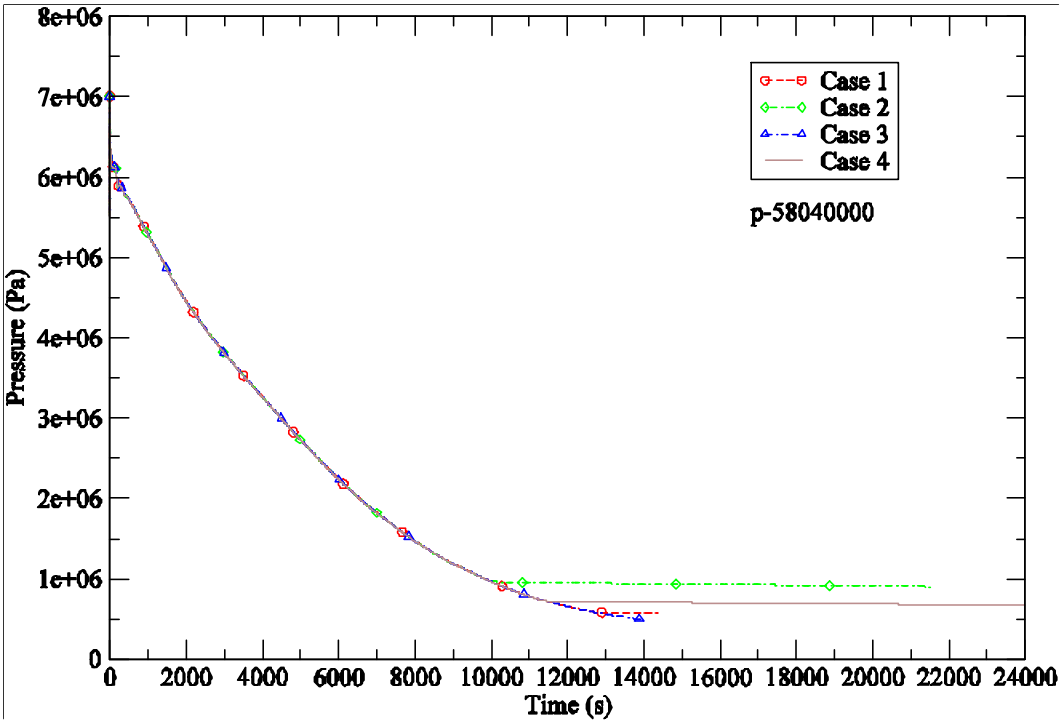

Figure 8 – Reactor pressure in the upper plenum.

the reactor pressure has dropped below 0.6MPa. If reliance on natural circulation cooling is delayed after a depressurization accident, e.g. by means of other active heat removal mechanisms such as battery powered blower, then natural circulation alone can become sufficient to removal decay power even at a guard containment pressure lower than 0.6MPa.

3.2.3 Guard Containment Pressure

There are several factors that determine the pressure build up in the guard containment after a leak in the reactor primary circuit. They are:

1. Initial state of the guard containment atmosphere, i.e. temperature, pressure, and volume.
2. Presence of heat structure to absorb sensible heat inside the guard containment.
3. Presence of active cooling device in the guard containment.
4. Through wall heat transfer to the outside.
5. Energy and mass transfer through the leak into the guard containment.

In Figure 9 the rate of pressure build up is seen to vary inversely with the assumed free volume of the guard containment. A peak pressure is reached when the combined heat removal from the Emergency Cooling System and heat conduction through the guard containment wall exceeds the decay power.

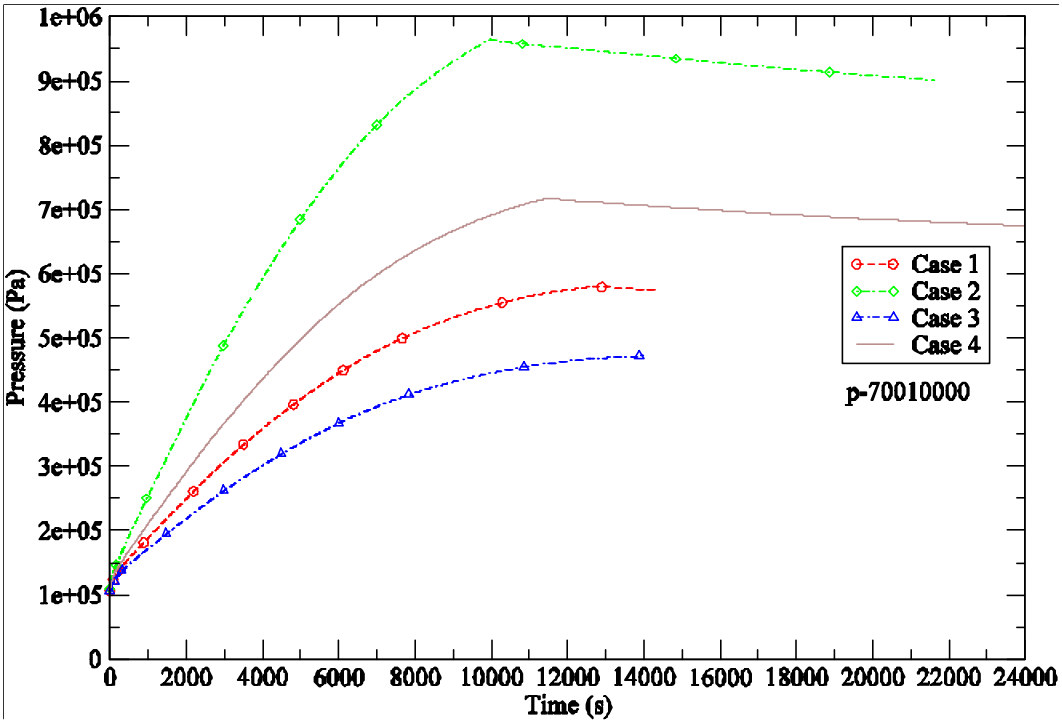

Figure 9 – Guard containment pressure.

It is noted that there are three means to mitigate the peak pressure inside the guard containment, by increasing the free volume, by venting the guard containment, and by using active heat removal. The viability of these means to minimize the peak pressure needs further evaluation.

3.2.4 Guard Containment Gas Temperature

The gas temperature of the guard containment increases rapidly after the initiation of the depressurization accident because of the relatively low heat capacity of its atmosphere. Figure 10 shows that the peak gas temperature varies inversely with the free volume of the guard containment. A high gas temperature is of concern not only for the environmental qualification of equipment and instruments inside the guard containment but also for the structural integrity of the support structures and the guard containment itself.

3.2.5 Hot Assembly Fuel Temperature

The general trend of the temperature transient experienced by the fuel is discussed with the aid of Figure 11 which shows the average temperature of the fuel node of the hot assembly near top of the core. The behavior of the fuel temperature is seen to be similar for all four parametric cases. The only difference is the attainment of a peak temperature for the two successful cases.

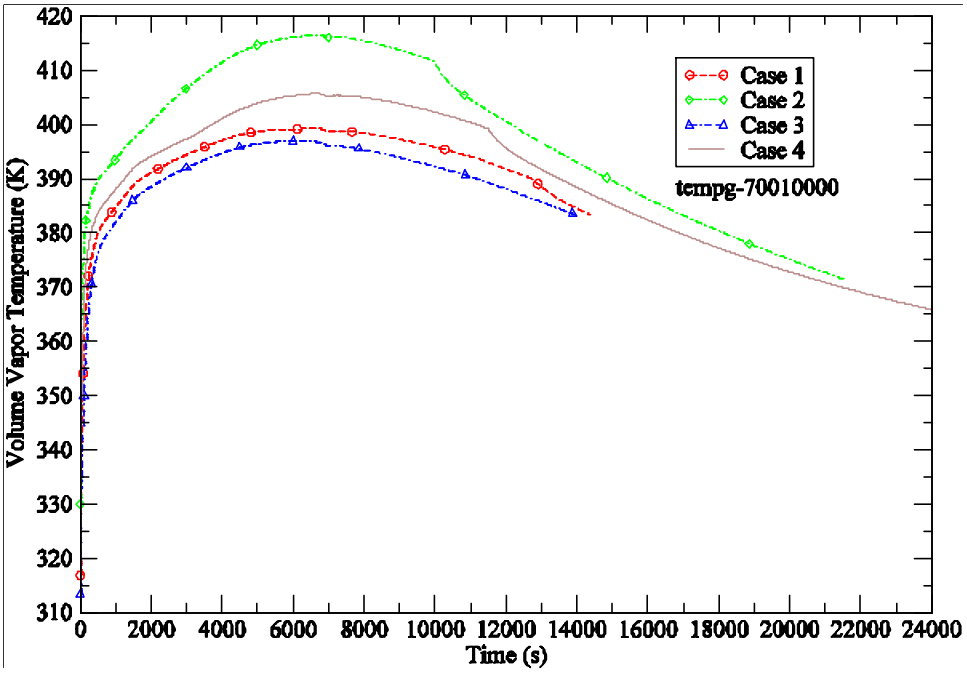

Figure 10 – Gas temperature inside the guard containment.

The initial drop in fuel temperature after the initiation of the transient is due to the rapid decrease in reactor power from operating level to decay heat level. The first temperature peak of slightly less than 1200K is from a combination of an increase in core inlet temperature (partly due to the approximate representation of the PCU in the current model) and a decrease in heat loss from the fuel when the flow from the PCU coasts down to zero. The duration of the coastdown has been found to be an important factor in deciding the magnitude of this first peak in fuel temperature. As natural circulation flow begins to develop through the core the rate of heat transfer from the fuel begins to increase again resulting in a decrease in fuel temperature. While the decay power is decreasing in time the natural circulation flow through the core is also slowing down because of loss in pressure through the leak. A minimum fuel temperature is reached at about 4000s into the transient and from that point on the fuel temperature begins an upward trend. With increasing fuel temperature the amount of heat transfer from the fuel into the flowing helium also increases. For the two success cases (Cases 2 and 4) the decay power eventually drops below the level that is sustainable by the helium flow and at a time before the fuel temperature limit is reached.

3.2.6 Maximum Fuel Temperature

Figure 12 shows the maximum fuel temperature as a function of time. It is obtained from the RELAP5/ATHENA results by defining a control variable that searches for the maximum temperature for all fuel heat structures at all axial locations. The behavior of the maximum fuel temperature is similar to the nodal temperature shown in Figure 11.

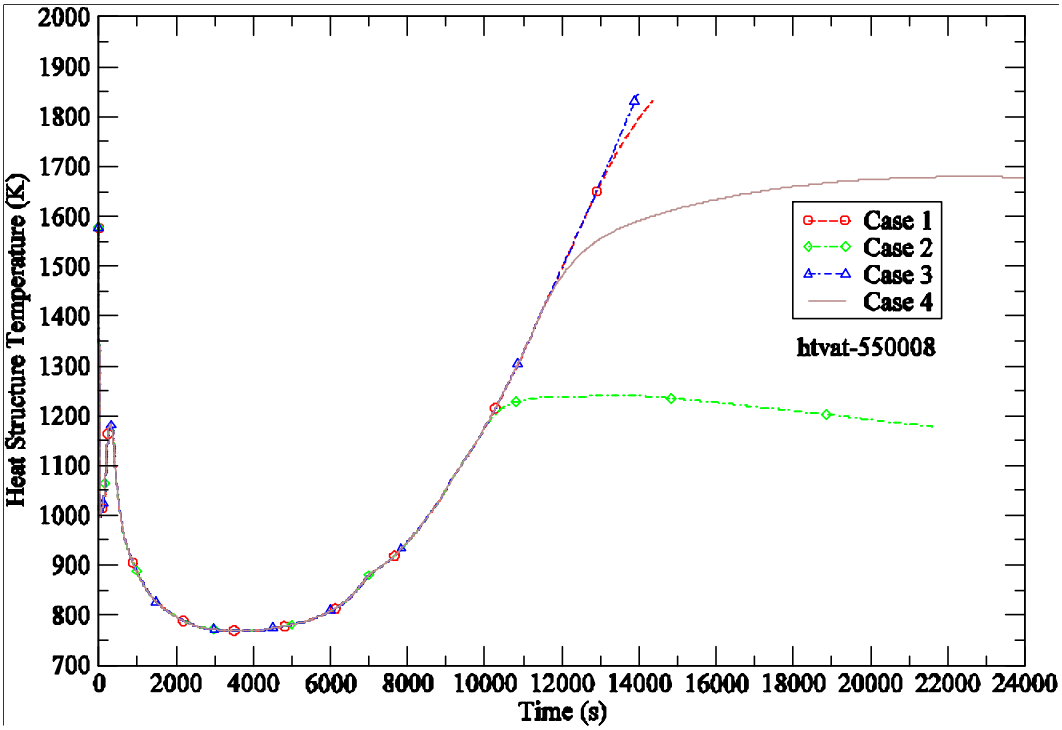

Figure 11 – Hot assembly fuel temperature near top of the core.

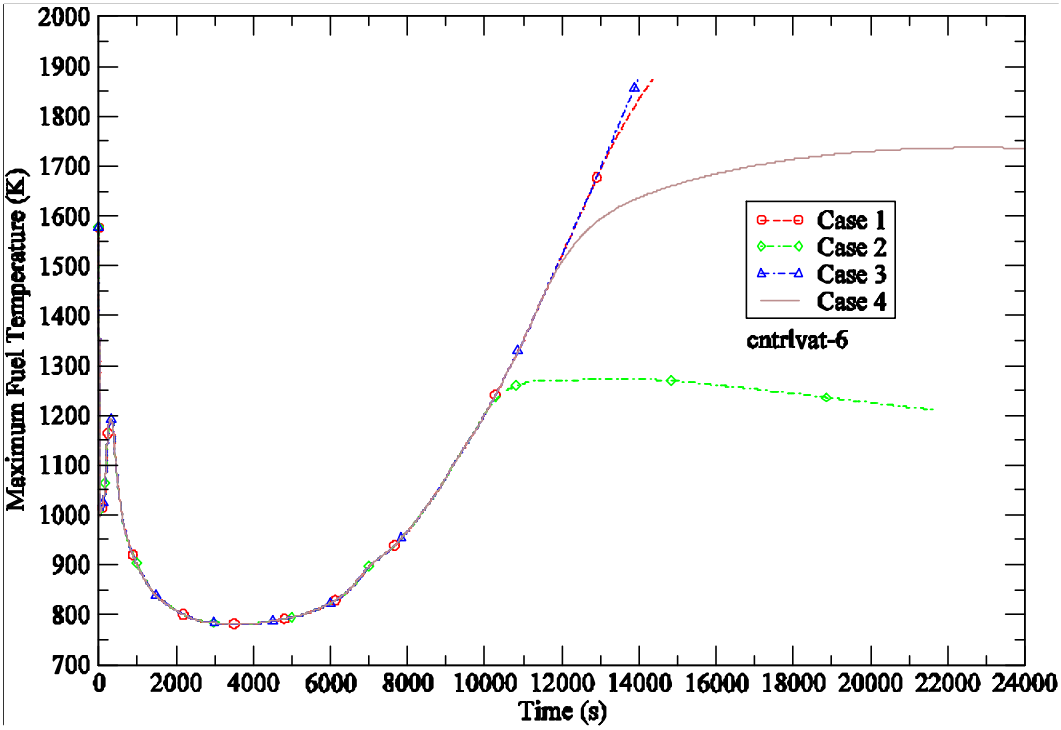

Figure 12 – Maximum fuel temperature core-wide.

3.2.7 Helium Flow in Natural Circulation

Natural circulation flow is established when the pressure difference across the check valve in the emergency heat exchanger loop has reached a threshold value. The helium flow rate shown in Figure 13 clearly demonstrates its dependence on the reactor pressure (see Figure 8). Higher flow rates are achieved at higher pressures. Based on economic and engineering constraints a maximum design pressure will be specified for the guard containment and that will have a direct bearing on the maximum passive heat removal rate achievable by natural circulation alone.

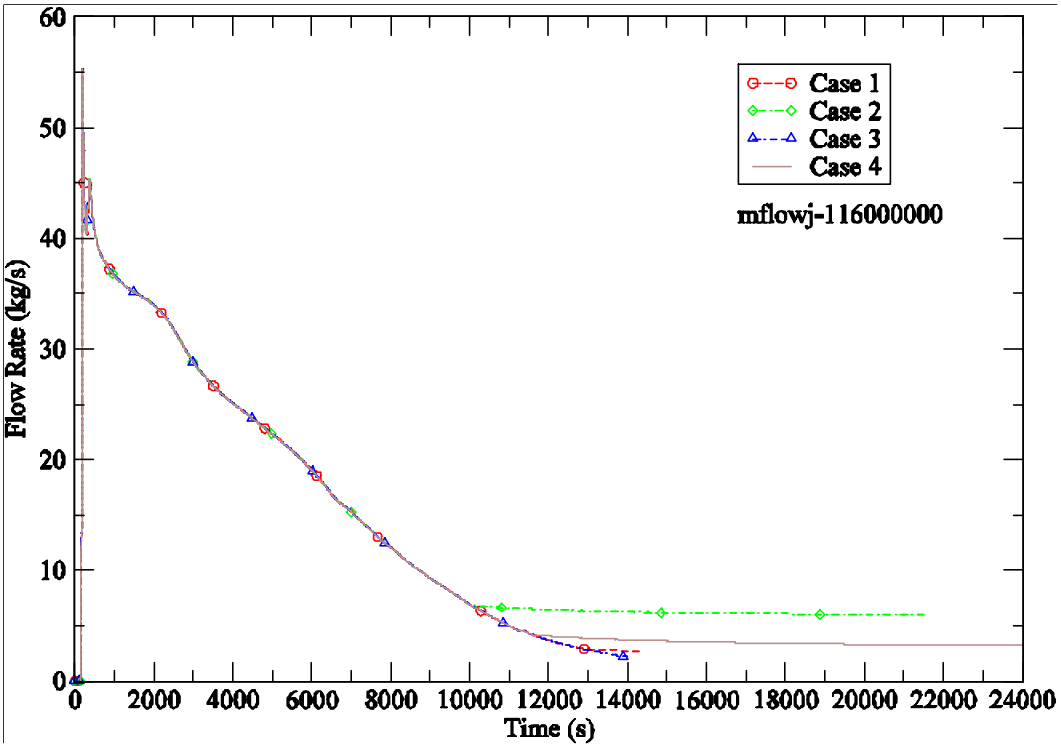

Figure 13 – Natural circulation flow rate of helium gas.

3.2.8 Gas Temperature at Core Outlet

The gas temperature at core outlet, shown in Figure 14, generally reflects the rate of heat transfer from the core to the helium flow. The progression of the core outlet temperature thus follows the trend of the fuel temperature shown in Figure 11.

3.2.9 Gas Temperature at Core Inlet

The initial surge in the core inlet temperature, shown in Figure 15, is somewhat unrealistic and is due to an approximation in the current PCU model discussed earlier in relation to the reactor pressure. In general the trend of the core inlet temperature corresponds to the difference between the heat removal rate of the emergency heat

exchanger and reactor power. A positive differential implies a decrease in core inlet temperature and vice versa.

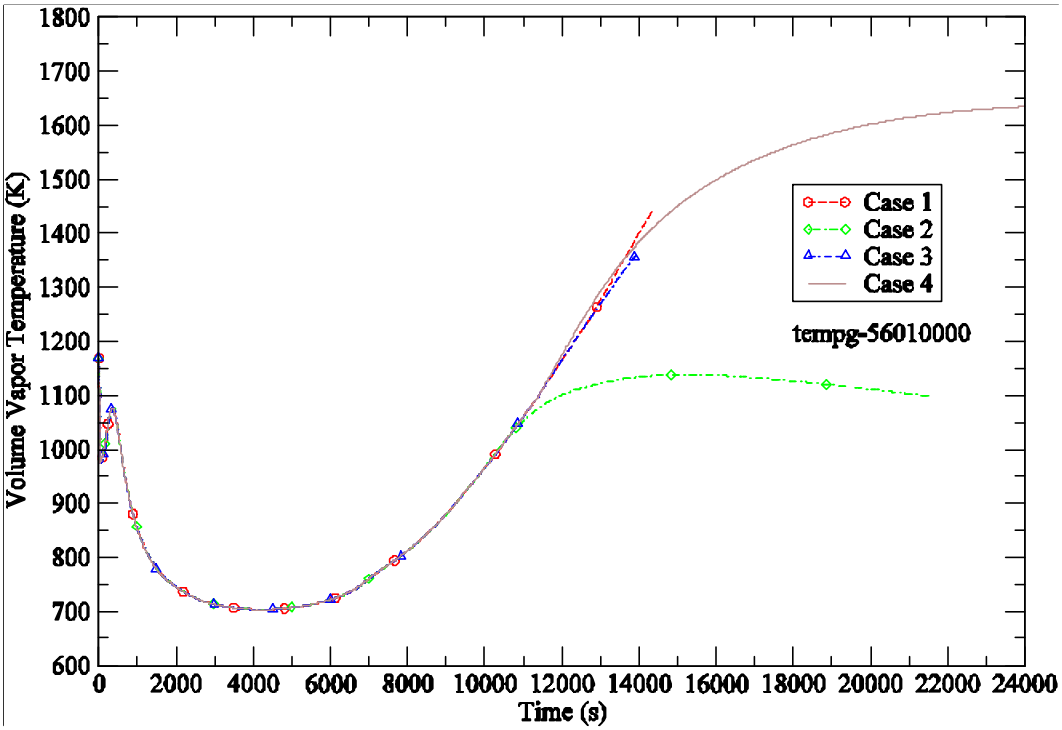

Figure 14 – Gas temperature at core outlet.

3.2.10 Water Flow Rate in the HEATRIC Heat Exchanger

The dynamic behavior of the water flow on the secondary side of the HEATRIC heat exchanger is shown in Figure 16 for flow at the inlet. The water flow is initiated by the commencement of helium flow on the primary side of the heat exchanger following the opening of the check valve. Since the water is initially stagnant a sudden influx of heat into the water channel prompted steam generation in the flow channel. The generation and collapse of steam voids in the water circuit create oscillations in the water flow. Eventually a stable natural circulation flow is established on the secondary side of the HEATRIC heat exchanger. Since water is incompressible a surge volume is needed to accommodate the thermal expansion of the flowing water. The variation of water flow rate among the parametric cases is small. Nonetheless qualitatively the result shows a higher water flow rate corresponding to a lower core inlet temperature (see Figure 15).

3.2.11 Water Temperature at the Outlet of the HEATRIC Heat Exchanger

The initial heat transfer to the water side is fairly high (see Figure 7) and this is reflected in the two-hundred-degree plus increase in the outlet temperature, as shown in Figure 17, a short time after flow has started in the heat exchanger. Changes in water temperature correspond to variations in the heat removal rate of heat exchanger. This indicates the operation of the secondary side is stable and follows the demand of the primary side.

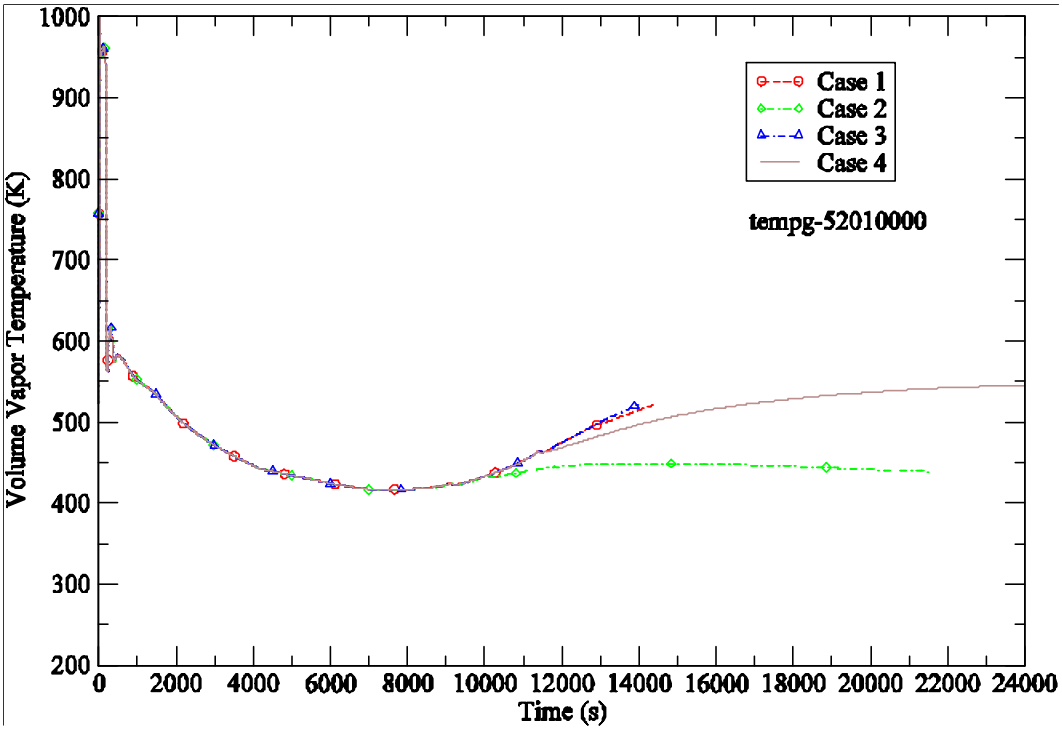

Figure 15 – Gas temperature at core inlet.

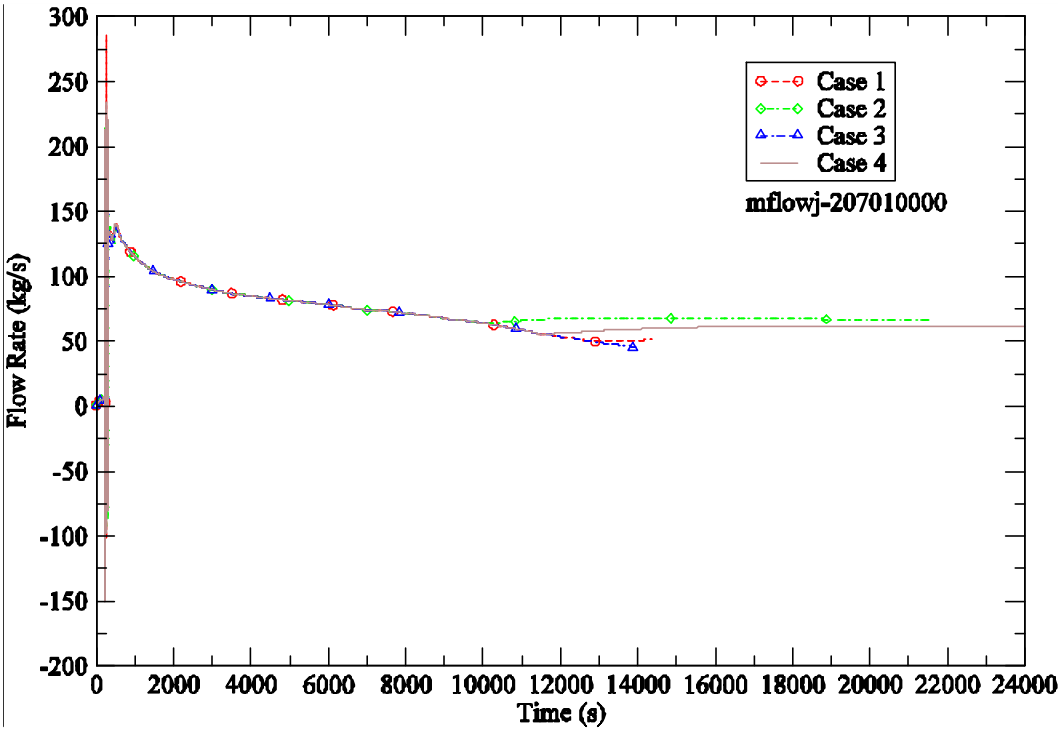

Figure 16 – Water flow rate in the HEATRIC heat exchanger.

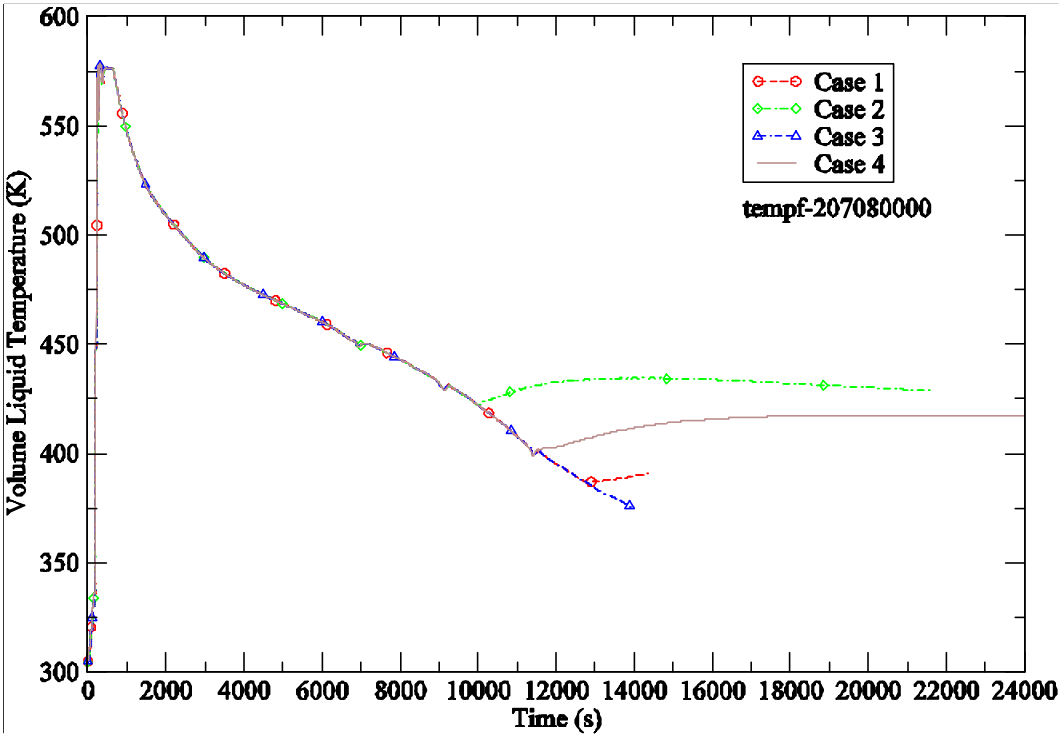

Figure 17 – Water temperature at the outlet of the HEATRIC heat exchanger.

3.2.12 Impact of Radiative Heat Transfer

The contribution of radiation heat transfer to the overall cooling of the fuel pins is demonstrated by the following tabulation that shows the energy balance for the upper half of the fuel pin in the hot assembly for Case 4 at the end of the calculation (24000s).

Heat Structure Node Number	Loss by Radiation (W)	Loss by Convection (W)	Power Source (W)	Net Loss of Power (W)
550006	12796	44351	56987	159.71
550007	14102	38994	52931	165.25
550008	11292	27168	38335	124.76
550009	6362	14334	20629	67.159

The heat structure temperatures and the coolant temperatures are shown below.

Heat Structure Node Number	Length of Node (m)	Fuel Temperature (K)	HEX Can Temperature (K)	Coolant Temperature (K)
550006	0.20205	1408.64	1378.97	1382.74
550007	0.20205	1567.93	1543.47	1546.71
550008	0.168381	1677.87	1658.29	1660.90
550009	0.101029	1735.77	1718.96	1721.17

The above tabulation shows that radiation accounts for 20-30% of the power loss from the fuel pin in the hot assembly. Radiation heat transfer becomes less significant for heat structures as their distance from the hot assembly is increased. The presence of unheated heat structures inside the reactor vessel increases the heat capacity of the system and this also helps to lower the heatup of the helium gas inside the vessel.

4.0 SUMMARY and CONCLUSIONS

The analysis of depressurization transient reported here for the 2400MW pin core design is an extension of an earlier analysis [4] for a 600MW core with half the power density of the current design (50W/cc versus the current 100W/cc). Major differences between the earlier analysis and the current one are in the fuel pin dimensions, the core power distribution, and the design of the emergency cooling system. In particular the emergency heat exchangers are now located ex-vessel and pressurized water is used as the working fluid on the secondary side. In addition radiation heat transfer is included in the current analysis.

The following conclusions can be drawn from this preliminary study:

1) With a 100W/cc core power density the sensitivity of maximum fuel temperature to core power distribution has pointed to the need of a more uniform core power distribution radially and axially.
2) Fuel pin design (pellet size, gap and clad thickness) also has a significant impact on the fuel temperature response in a depressurization accident.
3) In order to maintain the maximum fuel temperature within acceptable limits the guard containment pressure must, at least, be ~ 0.675 MPa. This pressure implies that the free volume of the guard containment can be no greater than 20,250 m^3.
4) Heat structures and radiative heat transfer are important phenomena in the post-accident thermal progression of the core. The effect of including these phenomena is to re-distribute the radial temperature profile compared to not including them. Briefly, the hot zones (fuel) are reduced in temperature, and the cold zones (reflector, shield

etc.) are increased in temperature relative to not including the above mentioned phenomena.

5) The coolant flow due to the coast down of the Turbine-Compressor-Generator (TCG) unit is an important factor in initially cooling the core following reactor scram, and in establishing the natural circulation flow. Currently this flow is approximated by linearly reducing the flow velocity to zero in 180 seconds. A more realistic model of this flow reduction (both mass flow rate and time) is required to make more accurate estimates of the maximum fuel temperature, and ultimately the guard containment volume. In order to carry out this more realistic calculation a complete Turbine Compressor model is required. This model will require the appropriate performance maps, inertia of the rotating parts, and some estimate of the internal friction of the blades rotating in the working fluid.
6) The emergency heat exchanger needs to be oriented in a vertical direction rather than horizontally, to avoid boiling of the pressurized water on the secondary side. The hot helium initially leaving the core causes the water on the secondary side to boil in the case of a horizontally oriented heat exchanger. This boiling induces flow oscillations, and potentially reverse flow on the secondary side, impeding the onset of natural circulation flow. These events are minimized in the case where the heat exchanger is oriented vertically, and the start of natural circulation flow proceeds smoothly.
7) Helium flow caused by either coast down or normal operation using emergency power supply (battery) of the ECS blower is not included in this calculation. This additional flow will help in establishing the natural circulation flow pattern following the start of the accident and also reduce the requirement of natural circulation cooling by prolonging the period of forced flow cooling. However, natural circulation flow is established in the current analysis, despite not including this flow. Thus, it would seem that including this flow is not crucial to cooling the core but its inclusion is necessary to create an accurate model of the accident progression.

5.0 REFERENCES

[1] "ATHENA Code Manual Volume I: Code Structure, System Models and Solution Methods," INEEL-EXT-98-00834, Revision 2.2, October 2003.

[2] Feldman, E. and Wei, T., "GFR Pin Core Designs for Passive Decay Heat Safety," I-NERI Project #2001-002-F Report GFR022, February, 2004.

[3] Personal Communication with Tom Wei of ANL, December 6, 2004.

[4] Cheng, L. and Ludewig, H., "Passive Decay Heat Removal Transient Analysis for Pin Core," I-NERI Project #2001-002-F Report GFR015, February, 2004.

TABLE 1. Reactor Vessel Geometry

Component	RELAP5 Volume #	Length (m)	Area (m^2)	H_D (m)
Upper Downcomer	047	3.241	6.775	0.61
Middle Downcomer	045 & 046 (in parallel)	4.5	3.3875	0.61
Lower Downcomer	050	7.627	6.775	0.61
Lower Plenum	051	2.68	33.65	6.71
Core Inlet	052	0.3	17.16	4.68
Average Zone	053	3.347*	6.2487	0.0122
Hot Zone	054	3.347*	0.9626	0.0122
Hot Assembly	055	3.347*	0.1050	0.0122
Core Outlet	056	0.5	17.16	4.68
Upper Plenum	058	11.5	35.36	6.71
Radial Reflector	032	3.347	0.0154	0.0122
Radial Shield	034	3.347	0.0103	0.0122

* Includes lower and upper reflectors – 1.0m each.

TABLE 2. PCU Geometry[#] and Initial Conditions

Component	Length (m)	Volume (m^3)	Area (m^2)	Orientation (Deg)	Hydraulic Diameter (m)
Hot Duct	7.4	11.88484921	1.6060607	0	1.43
Turbine	4.2	2.04	0.4857143	90	0.786404
Turb - Recu	1.3848	0.6924	0.5	-90	0.797885
Recuperator	2.8152	59.5	21.135266	-90	0.009164
Recu - Prec	10.95	5.475	0.5	-90	0.797885
Precooler	4.73	142.4	30.105708	-90	0.009164
LPC duct	4.9	11.78588119	2.4052819	90	1.75
LPC inlet	2.38	14.23918074	5.982849	90	2.76
LPC	4.2	2	0.4761905	90	0.778656
LPC outlet	4.9	21.3	4.3469388	-90	2.352593
Intercooler	4.73	139.8	29.556025	-90	0.009164
Intc - HPC	9.63	4.815	0.5	90	0.797885
HPC	4.2	2	0.4761905	90	0.778656
HPC-Recu	2	1	0.5	0	0.797885
Recuperator	2.8152	59.5	21.135266	90	0.009164
Recu - Cduct	2.8152	1.4076	0.5	-90	0.797885
Cold Duct	7.4	13.94867138	1.8849556	0	0.6
Total Volume		493.7885825			

Geometry is for one 600MW unit.

Component	Volume Nodes	Temp (C)	Temp (K)	Pressure (MPa)
Hot Duct	1-4	848	1121.15	7.07
Turbine	5-7	678	951.15	4.84
Turb - Recu	8	508	781.15	2.61
Recuperator	9-10	319	592.15	2.59
Recu - Prec	11-13	130.3	403.45	2.58
Precooler	14-17	78.3	351.45	2.56
LPC duct	18-19	26.4	299.55	2.55
LPC inlet	20	26.4	299.55	2.55
LPC	21-23	66.9	340.05	3.43
LPC outlet	24-25	107.5	380.65	4.31
Intercooler	26-29	66.8	339.95	4.29
Intc - HPC	30-32	26	299.15	4.28
HPC	33-35	68.2	341.35	5.76
HPC-Recu	36	110.3	383.45	7.24
Recuperator	37-38	299	572.15	7.2
Recu - Cduct	39-40	488	761.15	7.16
Cold Duct	41-44	488	761.15	7.16

TABLE 3. Properties of Fuel and Clad for the Pin Core

Fuel – UC

Density = 13.61×10^3 kg/m^3

Thermal Conductivity = 21.6 W/m-K

Specific Heat = 201 J/kg-K

Clad - SiC

Density = 3210 kg/m^3

Thermal Conductivity:

Temperature (K)	Thermal Conductivity (W/m-K)
673	25.12
873	21.77
1073	18.42
1273	16.12
1473	13.40

Specific Heat:

Temperature (K)	Specific Heat (J/kg-K)
600	1050
900	1170
1200	1250
1500	1320

ATTACHMENT 1

Input Data for the Emergency Cooling System (ECS) and the HEATRIC Heat Exchanger (HX)

Geometry of ECS

Notes:

(1) Loop dimensions are based on 'Database for MIT Design' (Database2400.xls, Pavel Hejzlar, 9/16/04).
(2) General layout of components is based on Hejzlar's presentation in Idaho, in May 2004 (viewgraph 20, Indirect cycle – Option IC2 (2))
(3) Flow areas are the sum of 2x50% loops. Each 50% loop has a capacity of 24MW.

HELIUM LOOP OF ECS

Inner Coax Duct (hot leg from RPV to SCS/ECS pod):
ID = 1.2m = D_H
Length = 4m
Orientation = horizontal
Flow Area = 2x π x$1.2^2/4$ = 2x1.131 = 2.262 m^2
K_{loss}:
Entrance = 0.23 and exit = 1.0.

Outer Coax Duct (cold leg, from SCS/ECS pod to RPV):
D_H = 0.3m (annulus with ID = 1.2m and OD = 1.5m)
Length = 3m
Orientation = horizontal
Flow Area (annulus) = 2x π x $(1.5^2-1.2^2)/4$ = 2x0.6362 =1.272 m^2
K_{loss}:
Entrance = 0.35, exit = 0.65 since diffuser like ending is used to reduce exit loss.

Lower HX Riser:
D_H = 1.8m
Length = 2m
Orientation = vertical (up)
Flow Area = 2x 3.24 = 6.48 m^2
Junction loss = abrupt area change (inner duct to lower HX riser)

Upper HX Riser:
D_H = 1.636m
Length = 5.5m (same height as the HEATRIC HX)
Orientation = vertical (up)
Flow Area = 4x 2.7 = 10.8 m^2
K_{loss} = 0.1 – flow split loss as lower riser splits into 2

The following assumptions apply to the HX inlet plenum, heat exchanger, and HX outlet plenum:

HX plates are stacked with alternate layers of helium and water flow channels.
Total channel flow area = no. of channels x 5mm-diameter half circle.

No. of hot channels in each 24MW HX = 306116
Channel length = 0.3m
Within each HX plate, the flow channels are connected at each end to an inlet and outlet plenum respectively. Consider these plenums as flow manifolds. Each plenum has a length equal to the width of a submodule (0.6m) and occupies an area that extends beyond the flow channels by 0.3m and a height of 0.0025m (height of a flow channel).

Flow area of one mini-inlet-plenum = 0.0025x0.6 (width of a submodule) = $0.0015m^2$
Flow area of one mini-outlet-plenum = 0.0025x0.3 (length of plenum) = $0.00075m^2$
No. of hot (cold) mini-plenums for each submodule = No. of hot (cold) plates in each submodule.
No. of hot plates in each submodule = 743.

HX Inlet Plenum:
D_H = 4x0.0015/ (2x (0.0025+0.6)) = 0.005m
Length = 0.3m
Orientation = horizontal
Flow Area = 8x743x0.0015 = 8.92 m^2
Junction loss = abrupt area change

Heat Exchanger:
D_H = 0.003055m
Length = 0.3m
Orientation = vertical[#]
Flow Area = 2x 306116 x π x0.005^2/8 = 2x306116x9.817x10^{-6} = $6.011m^2$
K_{loss}:
Entrance = 0.23 and exit =1.0

HX Outlet Plenum:
D_H = 4x0.00075/ (2x (0.0025+0.3)) = 0.005m
Length = 0.3m
Orientation = vertical[#]
Flow Area = 8x743x0.00075 = 4.46 m^2
K_{loss} = 1.0 (exit loss)

Blower/Check Valve Cavity:
There are 4 such cavities in each pod.
ID = 1.4m = D_H
Length = 4.9m + 1m for blower
Orientation = vertical
Flow area = 8x π x1.4^2/4 = 8x1.539 = 12.32 m^2
K_{blower} = 10 (locked blower)
K_{ch_v} = 3.23 (located at bottom of cavity)

[#] Original design had a horizontal orientation.

Lower HX Downcomer:
D_H = 2.026m
Length = 1m
Orientation = vertical (down)
Flow Area = 4x5.497 = 21.99m^2

Outer Coax Duct (cold leg, from SCS/ECS pod to RPV):
D_H = 0.3m (annulus with ID = 1.2m and OD = 1.5m)
Length = 3m
Orientation = horizontal
Flow Area (annulus) = 2x π x (1.5^2-1.2^2)/4 = 2x0.6362 =1.272 m^2
K_{loss}**:**
Entrance = 0.35, exit = 0.65 since diffuser like ending is used to reduce exit loss.

<u>WATER SIDE OF HX</u>

Coolant Inlet (cooling water from dump HX):
HX modules (each having 4 submodules) occupy a 1.8x1.8 square in the center of an SCS/ECS pod.
Width of each submodule is 0.6m
Space between 2 submodules is 1.8 – 2x0.6 = 0.6m
Inlet flow area = 2x0.6x0.9 = 1.08m^2

Coolant Outlet (cooling water from HEATRIC HX to dump heat exchanger):
Flow area occupies the two semi-circle areas on each side of the coolant inlet area.
Flow area = 2x (π x0.6^2/4 + 2x0.6x0.45) = 1.65 m^2 (sum of 2 semi-circles and 2 rectangles)

There is also a similar arrangement of inlet, outlet mini-plenum and cooling channels as for the helium side.

HEATRIC HX Layout for SCS/ECS Application (HP in will be our water line in and HP out will be water lines out). LP in and LP out is helium in and out. The box is 1.8mx1.8m.

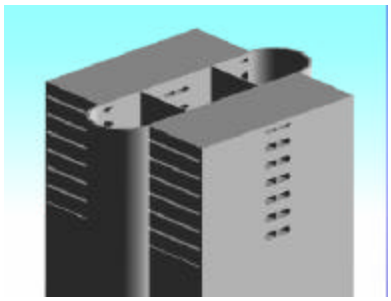

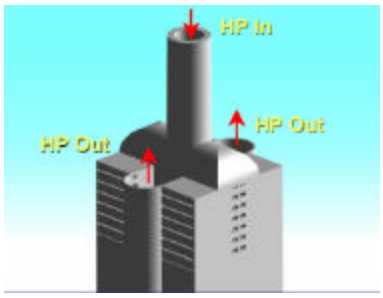

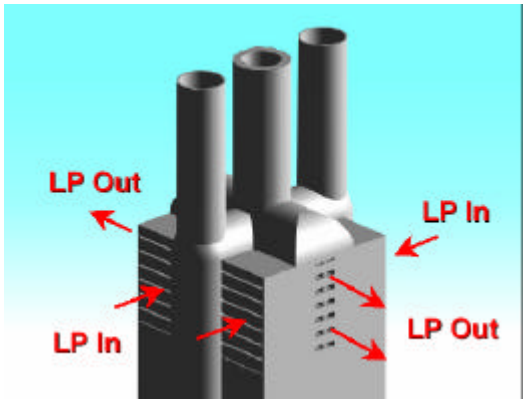

g)

Submodule layout

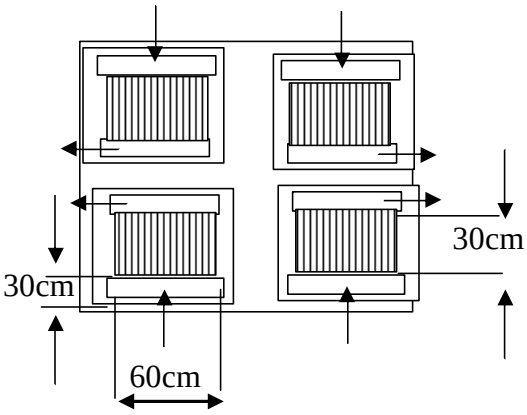

Channels are horizontal and fully countercurrent

Note: This sketch from Pavel Hejzlar (e-mail, 9/22/2004) shows the layout of the HEATRIC submodules for one heat exchanger unit. The original design had counter-current flow channels oriented horizontally. For reasons explained in the main text a vertical flow channel orientation was assumed for the calculations presented in this report.

Page from 'Database2400.xls' (e-mail from Pavel Hejzlar, 9/16/04)

Database for MIT Design

General Primary System Geometry (4 loops with 50% capacity each)

1	Lower Plenum	1	7400	1000	500	0.00	4.50E-05	43.00840343
2	Inlet Reflector	111021	12.2	1000	1000	0.80	1.00E-05	8.16062E-05
3	Active Core	111021	12.2	1340	1340	0.50	1.00E-05	8.16062E-05
4	Outlet Reflector	111021	12.2	1000	1000	1.50	1.00E-05	8.16062E-05
5	Lower Chimney	1	7400	3000	3000	0.00	4.50E-05	43.00840343
6	Upper Chimney	1	5400	6000	6000	0.10	4.50E-05	22.90221044
7	Inner Coax Duct	4	1200	4000	0	1.23	4.50E-05	1.130973355
8	Lower HX Riser	4	1800	2000	2000	0.00	4.50E-05	3.24
9	Upper HX Riser	8	1636	1500	1500	0.10	4.50E-05	2.7
10	HX Inlet Plenum	8	150	1250	-500	0.23	4.50E-05	0.67376
11	Heat Exchanger	612232	3.055	300	-300	1.23	1.00E-05	9.81E-06
12	HX Outlet Plenum	8	150	1250	-200	1.00	4.50E-05	0.67376
13	Upper HX Downcomer	8	2026	1000	-1000	0.00	4.50E-05	5.497477042
14	Blower/Check Valve	16	1400	3000	-3000	3.23/13.23	4.50E-05	1.5393804
15	Lower HX Downcomer	8	2026	1000	-1000	0.00	4.50E-05	5.497477042
16	Outer Coax Duct	4	300	3000	0	1.00	4.50E-05	0.636172512
17	Upper Downcomer	4	2025.33	5400	-5400	0.50	4.50E-05	2.290818003
18	Lower Downcomer	1	600	7340	-4940	1.00	4.50E-05	7.25707903
						0.00E+00		

General Description

4 x 50% Passive/Active Decay Heat Removal System with coaxial ducting and blowers. Primary gas coolant (Helium or CO2) and water secondary coolant x 33% blower per loop. Core Power Density is 100 kW/

Operation Parameters for 2 x 50%

Cold Shutdown	
Inlet Temperature	125.81 C
Outlet Temperature	850 C
System Pressure	1.83 Mpa
Decay Heat (2% total)	48 MW
Mass Flow Rate	12.60 kg/s
Pressure Losses	198.3 Pa
Refueling Shutdown	
Inlet Temperature	47 C
Outlet Temperature	250 C
System Pressure	0.5 Mpa
Decay Heat	12 MW
Total Blower Power	4.33 kW
Mass Flow Rate	11.26 kg/s
Pressure Losses	329.8 Pa
Primary Depressurization	
Inlet Temperature	123.91 C
Outlet Temperature	1000 C
System Pressure (Containment)	0.1 Mpa
Decay Heat	48 MW
Total Blower Power	241.5 kW
Mass Flow Rate	10.42 kg/s
Loop Pressure Losses	2911.3 Pa
Common Secondary System	
Heat Sink Constant	40 C refuel
Wall Temperature	107 C otherwise

Description of Heat Exchanger

Heat exchanger is a Heatric design PCHE. The chann are 5mm semi-circular. This is encased in the 5 m diameter heat exchanger pod.

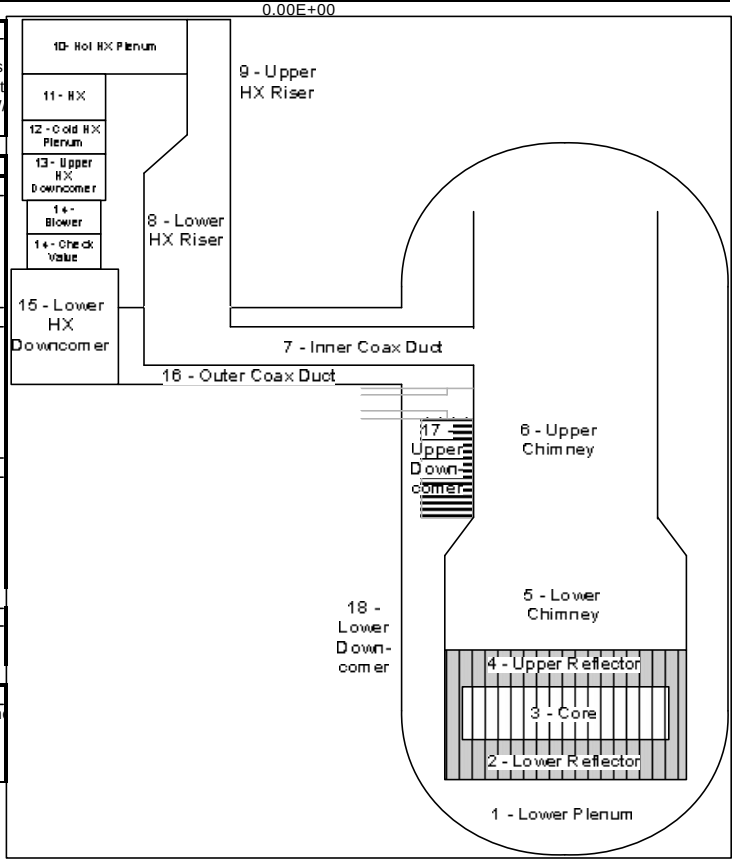

ATHENA INPUTS FOR PRIMARY SIDE OF ECS LOOP
(Helium Loop)

Component	Length (m)	Area (m^2)	H_D (m)	Junction Loss Coefficient
Inner Coax Duct	4 (H) 7.8265 (U)	2.262	1.2	0.23 (E) 1.0 (X)
Lower HX Riser	2.0 (U)	6.48	1.8	0.1 (Flow split loss)
Upper HX Riser	5.5 (U)	10.8	1.636	
HX Inlet Plenum	0.3 (H)	8.92	0.005	0.23 (E)
HX Flow Channel	0.3 (D)	6.01	0.003055	0.23 (E) 1.0 (X)
HX Outlet Plenum	0.3 (D)	4.46	0.005	1.0 (X)
Blower Cavity	5.9 (D)	12.32	1.4	10.0 (Locked blower)
Check Valve	-	12.32	-	3.23 (Valve loss)
HX Lower Downcomer	1.0 (D)	21.99	2.026	
Outer Coax Duct	7.8265 (D) 3.0 (H)	1.272	0.3	0.35 (E) 0.65 (X)

Orientation:

(H) = horizontal
(U) = up
(D) = down

Loss Coefficient:

(E) = Entrance
(X) = Exit

ATHENA INPUTS FOR SECONDARY SIDE OF ECS LOOP
(Water Loop)

Component	Length (m)	Area (m^2)	H_D (m)	Junction Loss Coefficient
Tube-side of Secondary HX	3.21 (H) x 10[#] 1.0 (D) x 9[##]	0.09649	0.03505	Abrupt area change
Pipe from Secondary HX	1.25 (D)	0.0873	0.333	Abrupt area change
Coolant Inlet of Primary HX	5.5 (D)	1.08	0.72	
HX Inlet Plenum	0.3 (H)	4.46	0.005	0.23 (E) 1.0 (X)
HX Flow Channel	0.3 (U)	6.01	0.003055	
HX Outlet Plenum	0.3 (U)	4.46	0.005	0.23 (E)
Coolant Outlet of Primary HX	4.9 (U)	1.65	0.674	Abrupt area change
Inlet Pipe to Secondary HX	10.25 (U) 3.0 (H)	0.0873	0.333	

10 tube passes where heat transfer occurs.
9 bends, one after each tube pass. No heat transfer is modeled in the bends.

Orientation:

(H) = horizontal
(U) = up
(D) = down

Loss Coefficient:

(E) = Entrance
(X) = Exit